CRC Report No. A-75-2

Modeling Europe with CAMx for Phase II of the Air Quality Model Evaluation International Initiative (AQMEII)

Final Report

May 2011

COORDINATING RESEARCH COUNCIL, INC.
3650 MANSELL ROAD·SUITE 140·ALPHARETTA, GA 30022

The Coordinating Research Council, Inc. (CRC) is a non-profit corporation supported by the petroleum and automotive equipment industries. CRC operates through the committees made up of technical experts from industry and government who voluntarily participate. The four main areas of research within CRC are : air pollution (atmospheric and engineering studies); aviation fuels, lubricants, and equipment performance, heavy-duty vehicle fuels, lubricants, and equipment performance (e.g., diesel trucks); and light-duty vehicle fuels, lubricants, and equipment performance (e.g., passenger cars). CRC's function is to provide the mechanism for joint research conducted by the two industries that will help in determining the optimum combination of petroleum products and automotive equipment. CRC's work is limited to research that is mutually beneficial to the two industries involved, and all information is available to the public.

Foreword

Under CRC Project A-75-2 "Modeling Europe with CAMx for Phase II of the Air Quality Model Evaluation International Initiative (AQMEII)," ENVIRON International Corporation collaborated with researchers from Europe (from INERIS in France and the University of Athens in Greece) to model ozone and particulate matter (PM) for Europe in 2006. The modeling was performed as part of the AQMEII study organized by the European Commission's Joint Research Centre (JRC) and the United States Environmental Protection Agency (EPA) to promote research and collaboration between scientists in Europe and North America on regional air quality model evaluation. The results from A-75-2 are presented in the format of a draft journal manuscript. The manuscript prepared under CRC Project A-75-1 has been expanded by including results of sensitivity tests to model inputs and assumptions and analysis of ozone sensitivity to precursor emissions. The expanded manuscript will be submitted to a special issue of Atmospheric Environment devoted to the AQMEII study.

The draft manuscript is included in this report along with an Executive Summary and supporting materials for the journal article.

Draft Final Report

CRC PROJECT A-75-2

Modeling Europe with CAMx for Phase II of the Air Quality Model Evaluation International Initiative (AQMEII)

Prepared for

CRC Atmospheric Impacts Committee
Coordinating Research Council
3650 Mansell Road, Suite 140
Alpharetta, GA 30022

Prepared by

Uarporn Nopmongcol
Bonyoung Koo
Edward Tai
Jaegun Jung
Piti Piyachaturawat
Chris Emery
Greg Yarwood
ENVIRON International Corporation
773 San Marin Drive, Suite 2115
Novato, CA 94998

Guido Pirovano
Christina MItsakou
Institut National de l'Environnement Industriel et de Risques (INERIS)
Paris, France

George Kallos
School of Physics, the Division of Physics of Environment and Meteorology
University of Athens, Greece

May 2, 2011

Executive Summary

The Comprehensive Air Quality Model with Extensions (CAMx) photochemical grid model was used to model ozone (O_3) and particulate matter (PM) for most of Europe in the framework of the Air Quality Model Evaluation International Initiative (AQMEII) phase I. The AQMEII study is organized by the European Commission's Joint Research Centre (JRC) and the United States Environmental Protection Agency (EPA). The aims are to promote research and collaboration between scientists in Europe and North America on regional air quality model evaluation. AQMEII provided input data for 2006 emissions, meteorology and boundary conditions (BCs) and requested that participants simulate one year of air quality for Europe and/or North America using AQMEII input data where possible. The AQMEII project is evaluating the resulting ensembles of model results for each continent. For this purpose, ENVIRON interpolated the CAMx results onto a specified analysis grid and transferred them to JRC for statistical and graphical evaluation using a software system called ENSEMBLE The objective is to provide consistent analysis methods and enable evaluation of the ensemble predictions of all models. ENVIRON also performed an independent evaluation of the CAMx modeling results.

The previous report for CRC project A 75-1 discussed ENVIRON's application of CAMx to Europe using the input data provided by AQMEII. This report for project CRC A 75-2 discusses model sensitivity analyses to investigate the influence of input data, assumptions and uncertainties on model performance using the CAMx application described in the previous report. Multiple simulations were conducted to identify the role played by different input data and assumptions. Alternate inputs and model configurations tested include BCs from alternate global models (GEOS-Chem and MOZART), meteorological conditions from WRF, reduced MEGAN isoprene emissions, modified vertical distributions for fire and shipping emissions, and alternate deposition (Wesely/Slinn) and chemistry (CB6) schemes. Model performance for January and July 2006 exhibited under-estimation trends for all pollutants both in winter and summer, except for SO_2. SO_2 generally had little bias although some over-estimation occurred at coastal locations and this was attributed to incorrect vertical distribution of emissions from marine vessels. However, sensitivity analysis using alternate vertical distribution of shipping emissions indicates that the model is insensitive to this change. It may be because the analysis is limited by the approach used to allocate ship emissions. Since it was not feasible to separate ship emissions in the TNO inventory from other mobile sources, only emissions in the open water grid cells were assumed to be from ships. Ship emissions at ports or along coastal waterways may not have been places at higher layer; as a result, the effects from ship could not be fully captured.

Alternate vertical distribution of fire emissions also had minor impacts on model performances. Performance for NOx and NO_2 was better in winter than summer. The tendency to under-predict daytime NOx and O_3 in summer may result from insufficient NOx emissions or overstated daytime dilution (e.g., too deep planetary boundary layer). WRF meteorology significantly improved NOx performance, but O_3 performance got worse. Winter O_3 was biased low and this was attributed to a low-bias in the O_3 boundary conditions. Both MOZART and GEOS-Chem BCs appear to improve January O_3 performance significantly. PM_{10} was widely under-predicted in both winter and summer. The poor PM_{10} was influenced by under-estimation of coarse PM emissions. The Wesely/Slinn deposition scheme tended to increase ozone in winter and PM in both months. CB6 chemistry improves January O_3 and PM performances considerably. Reduced MEGAN isoprene emissions have relatively small impacts to model performance.

The higher-order decoupled direct method (HDDM) was applied to a two-week-long July episode to compute the first- and second-order ozone sensitivities to domain-wide anthropogenic NOx and VOC emissions. In central and southern Europe, anthropogenic NOx contributions are much higher than anthropogenic VOC contributions indicating that ozone formation is mostly NOx-limited. This is due to large biogenic VOC emissions in the region. Zero-out contributions and ozone isopleths were constructed using the HDDM sensitivity coefficients for several metropolitan areas and used to show the chemical regime (NOx-limited or VOC-limited) of ozone formation in the area. Ozone isopleths also showed how robust the chemical regime to uncertainties in the emission inventories.

Draft Journal Manuscript

Modeling Europe with CAMx for the Air Quality Model Evaluation International Initiative (AQMEII)

Uarporn Nopmongcol[a], Bonyoung Koo[a], Edward Tai[a], Jaegun Jung[a], Piti Piyachaturawat[a], Christ Emery[a], Greg Yarwood[a], Guido Pirovano[b,c], Christina Mitsakou[d], George Kallos[d]

[a] ENVIRON International Corporation, 773 San Marin Drive, Suite 2115, Novato, CA 94998, USA
[b] Ricerca sul Sistema Energetico (RSE), Italy
[c] Institut National de l'Environnement industriel et de risques (INERIS), France
[d] School of Physics, the Division of Physics of Environment and Meteorology, University of Athens, Greece

ABSTRACT

The CAMx photochemical grid model was used to model ozone and particulate matter over a European modeling domain for calendar year 2006 as part of the Air Quality Model Evaluation International Initiative (AQMEII). The CAMx base case utilized input data provided by AQMEII for emissions, meteorology and boundary conditions. Sensitivity of model outputs to input data was investigated by using alternate input data and changing other important modeling assumptions including the schemes to represent photochemistry, dry deposition and vertical mixing. Impacts on model performance were evaluated by comparisons with ambient monitoring data. Base case model performance for January and July 2006 exhibited under-estimation trends for all pollutants both in winter and summer, except for SO_2. SO_2 generally had little bias although some over-estimation occurred at coastal locations and this was attributed to incorrect vertical distribution of emissions from marine vessels. Performance for NOx and NO_2 was better in winter than summer. The tendency to under-predict daytime NOx and O_3 in summer may result from insufficient NOx emissions or overstated daytime dilution (e.g., too deep planetary boundary layer). Winter O_3 was biased low and this was attributed to a low-bias in the O_3 boundary conditions. PM_{10} was widely under-predicted in both winter and summer. The poor PM_{10} was influenced by under-estimation of coarse PM emissions. Sensitivities of ozone concentrations to precursor emissions are quantified using the decoupled direct method in CAMx. The results suggest that ozone production over the central and southern Europe during summer is mostly NOx-limited.

1. Introduction

The Comprehensive Air Quality Model with Extensions (CAMx) photochemical grid model (ENVIRON, 2010) was used to model ozone (O_3) and particulate matter (PM) for most of Europe in the framework of the Air Quality Model Evaluation International Initiative (AQMEII). Multiple

models were applied in the AQMEII and to promote consistent model applications and minimize uncertainties associated with use of differing inputs by each model, the AQMEII organizers made available key model input data such as emissions, boundary conditions (BCs) and meteorology. However, many models used different meteorological data, several used different BCs and a few are used different emissions. In this study, we investigated the influence of input data, assumptions and uncertainties on CAMx model performance for the European domain. In the following sections, we discuss the application of CAMx to Europe using the input data provided by AQMEII, model sensitivity analyses including use of alternate input data/assumptions, and ozone sensitivity to precursor emissions (anthropogenic NOx and VOC).

2. Methodology

2.1. Base Case Modeling

Air quality modeling for the European (EU) domain and calendar year 2006 used CAMx version 5.21 to simulate physical and chemical processes governing the formation and transport of ozone and PM (ENVIRON, 2010) with Carbon Bond 05 (CB05) gas phase chemistry (Yarwood et al., 2005). Model inputs were prepared from data provided by AQMEII supplemented by other data sources as described below. The CAMx modeling domain was defined in latitude and longitude with 207 by 287 grid cells and 23 vertical layers. The modeling domain covered most of Europe, from 15.875°W to 35.875 °E and 34.5625°N to 70.4375°N, with a grid resolution of 0.125° latitude by 0.25° longitude (equivalent to about 15 to 20 km). The grid resolution of the CAMx domain was aligned to the emission inventory in order to avoid spatial interpolation of gridded emissions data. The extent of the CAMx domain encompasses the common grid for analysis of model results, from 15°W to 35°E and 35°N to 70°N at 0.25° resolution.

2.1.1.Meteorology

Meteorological data for calendar year 2006 were developed for AQMEII using the MM5 model (Duhdia, 1993) with 35 km resolution by the Laboratoire des Sciences du Climat et de l'Environnement (CEA) in Paris, France (Vautard, 2010). The MM5 domain was defined in Mercator projection with 180 by 220 grid cells and 32 vertical layers with a 30 meter deep surface layer. The MM5CAMx preprocessor for CAMx was used to interpolate from the Mercator projection employed by MM5 to the more finely resolved latitude-longitude coordinate system used by CAMx. CAMx employed fewer vertical layers (23) than MM5 (32) to reduce the computational burden of the air quality simulations. The CAMx vertical layers exactly matched those used in MM5 for the lowest 14 layers (up to ~1,800

m) and above this altitude were aggregates of several MM5 layers. Minimum vertical diffusivity (K_v) was set to 1.0 m^2/s.

2.1.2.Emission inventory

Anthropogenic emissions for 2006 were developed by TNO Environment and Geosciences (Denier van der Gon, 2010). The data consisted of annual average emissions for 10 SNAP (Selected Nomenclature for sources of Air Pollution) sectors (Visschedijk et al., 2007) on a 1/16 by 1/8 degree latitude-longitude grid. Major point sources were gridded, which combined sources of the same SNAP sector in each grid cell, and plume rise was accounted using layer-fractions which were constant spatially and temporally for each SNAP sector. Chemical constituents included methane (CH_4), carbon monoxide (CO), nitrogen oxides (NOx), sulfur oxides (SOx), non-methane volatile organic compounds (NMVOC), ammonia (NH_3) and particulate matter of 10 and 2.5 micrometers or less (PM_{10} and $PM_{2.5}$).

The Emissions Processing System version 3 (EPS3) was used to prepare emissions data for input to CAMx using temporal allocation and vertical layer distribution profiles provided by TNO for each SNAP sector. Speciation profiles for NMVOC to the CB05 chemical mechanism (Yarwood et al., 2005) were developed based on data from Passant (2002). TNO provided PM speciation profiles to allocate PM10 to sulfate (PSO4), elemental carbon (EC), primary organic carbon (POC), Sodium (Na), other PM fine, and other PM coarse. CAMx models the total mass of organic aerosol (i.e., POA for primary organic aerosols) rather than carbon mass (i.e., POC) and factors of 1.45-1.8 were applied to the POC mass to calculate POA and subtracting the mass difference from "other PM fine" to conserve total PM mass.

The 2006 anthropogenic emissions for the CAMx modeling domain are summarized by SNAP sector in Table 1 and by country or sea area in Table S1. NOx emissions are primarily from on-road and off-road mobile sources (63%) which includes marine vessels. The largest contributor to SO_2 emissions (56%) is the power generation sector. Solvent use contributes 37% and on-road mobile sources (22%) of NMVOC emissions. Agricultural sources dominate NH_3 emissions (93%). Emissions in sea areas are dominated by commercial shipping.

Biogenic emissions depend strongly on meteorology and landcover and were estimated using the Model of Emissions of Gases and Aerosols from Nature (MEGAN; Guenther, et al., 2006; Sakulyanontvittaya, et al., 2008) at each hour for each grid cell. MEGAN has a global database of landcover derived from satellite data at 1 km resolution. Meteorological input data for MEGAN (i.e.,

temperature and solar radiation) were taken from the MM5 predictions. MEGAN estimates emissions of isoprene, methylbutenol, terpenes, sesquiterpenes, other VOCs (OVOCs) and soil NOx.

Biomass burning emissions were estimated by the Finnish Meteorological Institute (FMI; Sofiev et al., 2010) using the fire radiative power (FRP) data product from MODIS equipped satellites. The dataset consisted of daily PM emissions for each fire gridded at 0.1° resolution. Scaling factors were provided to calculate gaseous components (CO, HCHO, NOx, NH_3, and SO_2) as ratios to PM. FMI suggested distributing emissions vertically by placing 50% of emissions below 200 m and 50% between 200 m and 1 km (Sofiev et al., 2010) but US modeling studies have used higher plume rise (ASI, 2005). Plume rise is related to the spatial extent of fires, and other factors, which are likely to differ for the conditions analyzed by FMI and the US studies. For the base case, fire plume rise was modeled by analyzing the emission inventory data to categorize the area burned by each fire and then using plume rise equations specific for fires of differing spatial extent (ASI, 2005).

Emissions of sea-salt particles, including sodium, chloride, and sulfate (SO_4), were estimated from the MM5 hourly, gridded meteorology using flux equations for open ocean (Smith and Harrison 1998; Gong, 2003) and breaking waves in the surf zone (de Leeuw et al., 2000).

Average daily emissions in January and July 2006 for each source category are summarized in Table S2.

2.1.3.Boundary/Initial Conditions (BCs/ICs)

Boundary conditions (BCs) for the base case were from data provided by the European Centre for Medium-Range Weather Forecasts (ECMWF) GEMS project (http://gems.ecmwf.int). The GEMS data were a composite of two models, namely MOZART for gases and IFS for particles. EPA evaluated the GEMS BCs by comparison with climatological values and GEOS-Chem model results for North America (Schere, 2010) and concluded generally that differences between the three data sources were within the uncertainty ranges. However, EPA recommended not using sea-salt from GEMS because concentrations were high. The SO_2 and SO_4 data from GEMs also were not recommended as they were based on simple assumptions for emissions and removal rather than a complete atmospheric transformation mechanism. Neglecting sulfur from the boundaries should not greatly affect the simulations, since SO_2/SO_4 should be strongly forced by emissions within the domain. The GEMS data did not provide PM nitrate or ammonium. For the base case, BCs were extracted from GEMS data and formatted for CAMx. Background concentrations were assumed for

nitrate, ammonium, sulfate and other aerosol species missing from the GEMS data. The 2006 annual simulation was initialized on December 18, 2005, to limit the influence of the ICs on results for 2006.

2.2. Sensitivity Cases

Multiple sensitivity simulations were conducted to identify the role played by different input data and assumptions. Two one-month periods, January and July, were modeled for each sensitivity case and evaluated against measurements. Information on the alternative inputs and assumptions are provided below.

2.2.1.Boundary Conditions

To investigate the contrasting impacts of other data sources for BCs, we replaced the GEMS BCs with results from other global models, namely, GEOS-Chem v8–03–01 (Yantosca and Carougeand, 2010) and MOZART4.6 (Emmons et al., 2010). The 2006 GEOS-Chem simulation was performed by ENVIRON using input data provided by Harvard University while the 2006 MOZART results were from the University Corporation for Atmospheric Research (UCAR, 2010).

2.2.2.Meteorology

The MM5 meteorology was replaced with WRF meteorology provided by the University of Hertfordshire (Chemel, 2010). The WRF domain covers almost all of Europe using 269 by 249 grid cells at 18 km resolution. The projection is Lambert Conformal. The vertical domain definition has 51 vertical layers with an approximately 25 meter deep surface layer. The WRF data was collapsed to 24 layers in CAMx and interpolated to the CAMx lat-lon grid. Two sensitivity tests were performed using WRF meteorology with different minimum vertical diffusivity (K_v) values of 0.1 or 0.04 m^2/s. The major impact of changing the minimum K_v is on nighttime mixing in/out of the shallow surface layer in CAMx.

2.2.3.Emissions

Emission estimates by MEGAN are generally higher than those estimated by EPA's Biogenic Emission Inventory System model (Pouliot, 2008). A comparison against aircraft-based measurements suggested that MEGAN over-estimated isoprene by up to a factor of 2 (Warneke et al., 2010). A sensitivity test was conducted with the MEGAN isoprene emissions reduced by half.

As discussed above, biomass burning emissions in the base case were distributed vertically according to the plume rises reported in US studies (ASI, 2005). Satellite data analysis by FMI suggested lower

plume-rise, i.e., ~80% within planetary boundary layer (PBL) and most plumes are below 4 km (Sofiev et al., 2010). A sensitivity test was conducted using fire vertical profiles modified to conform better to these satellite data and FMI's recommendation.

Shipping emissions in the base case were placed in the first model layer following vertical profiles suggested by AQMEII. However, deep draft vessels which account for most of the shipping emissions have stack heights comparable to the 40 m depth of the lowest CAMx layer . A study for the Port of Los Angeles characterized the stack height for deep draft vessels as between 34 and 58 m above the waterline (SCG, 2004). A sensitivity test with shipping emissions over open water assigned 75% to the second CAMx layer (the second layer top is at 73 m.) and 25% to the first CAMx layer. However, because emissions from shipping were combined with other mobile sources, this sensitivity adjustment was applied only for grid cells characterized as 100% water meaning that in-port emissions from deep draft vessels were still assigned entirely to the surface layer.

2.2.4.Dry Deposition

CAMx offers two dry deposition options: the original approach is based on the work of Wesely (1989) for gases and Slinn and Slinn (1980) for particles; and a more recent approach is based on the work of Zhang et al. (2001; 2003). The base case used the Zhang scheme with 26 landuse categories and incorporates vegetation density effects via leaf area index (LAI) to scale pollutant uptake into biota. The Wesely/Slinn model is formulated for 11 landuse categories. A sensitivity test was conducted using the Wesely/Slinn scheme.

2.2.5.Gas-Phase Chemistry

The gas-phase chemical mechanism strongly influences model predictions for oxidants and secondary PM. A sensitivity test implemented the Carbon Bond 6 (CB6) chemical mechanism (Yarwood et al., 2010) with the rate constant for OH and NO_2 measured by Mollner et al. (2010). Changes in CB6 compared to CB05 include reactions of aromatics, isoprene, ketones and production of HO_2 radical from RO_2 radicals. CB6 was used with the CB05 modeling inputs which means that some improvements (e.g., explicit treatments of propane, benzene and acetylene) were not exploited.

3. Performance Evaluation

Model performance was evaluated using methods implemented in the Atmospheric Model Evaluation Tool (AMET; Appel et al., 2010).

Ambient air quality measurements from the AirBase database for Europe (EEA, 2010) were used with AMET to compute statistical metrics of model performance. Background monitors (i.e., reported as being removed from traffic and industrial sources) below 700 m elevation and with data availability exceeding 75% were included in this analysis (~ 1,400 sites). The AirBase system classifies monitors according to location type with most of the selected stations classified as urban background, 379 as suburban background and 360 as rural background. Statistical metrics for PM constituents were computed using data from the European Monitoring and Evaluation Program (EMEP) database (EMEP, 2010). Monthly normalized mean bias (NMB), normalized mean error (NME), fractional bias (FB) and fractional error (FE) statistics (Table 2) were calculated for January and July using paired predictions and observations. Concentration thresholds were applied to the observed data (i.e., NOx $\geq$ 0.5 ppb, $NO_2 \geq$ 0.5 ppb, $O_3 \geq$ 5 ppb, $SO_2 \geq$ 0.2 ppb, CO $\geq$ 10 ppb, $PM_{10} \geq$ 1.0 µg/m3) to focus on conditions that exceed measurement thresholds. Table 3 reports the statistical performance metrics over all stations in the modeling domain for January and July 2006.

Overall, the base case simulation under-predicted all species except SO_2 in both January and July (Table 3). SO_2 has less than 10% bias (NMB and FB) in both months but greater than 60% error (NME and FE) indicating that the average concentrations are predicted correctly but with substantial scatter. For O_3 and CO, model performance improves in July compared to January. NOx, NO_2 and PM_{10} are substantially underestimated and performance is poor for both months with similar magnitude bias and error statistics indicating that the underestimation trends are consistent both spatially and temporally. Analyzing the MNB and FB statistics for January by monitor location type (Table S3) shows less under-prediction tendency at rural monitors than at urban monitors for most species except O_3. January O_3 is under-predicted for both the rural and urban monitor types.

The diurnal cycle of July O_3 (Figure S1 (a)) shows that the model reproduces well the daily modulation in O_3. In contrast to July, January O_3 performance is poor showing consistent under-predictions. The diurnal cycle of January O_3 (Figure S1 (a)) shows that the model reproduces the daily modulation in O_3 but with an offset due to a consistent low bias. Since O_3 production by atmospheric chemistry is generally suppressed in winter, O_3 transport from the model boundaries (i.e., BCs) is expected to be the dominant factor in causing the low bias for O_3 in January. Both MOZART and GEOS-Chem BCs improve January O_3 performance significantly with the FB bias decreasing from 63% (base case) to 0.2% (MOZART) and 21% (GEOS-Chem) (Table 3). The effects of changing BCs are less evident in July and at urban stations.

In contrast to O_3, NOx performance is fairly good at rural background stations in January (Table S3). In July, CAMx predicted much lower day-time NOx than observed (Figure S2 (a)). These problems may stem from insufficient NOx emissions or overstated daytime dilution (e.g., too deep planetary boundary layer) of NOx emissions in July. WRF meteorology has high impacts to model performance in both months, particularly to NOx. NOx has less than 13% low bias (NMB and FB) compared to 75% low bias (FB) in the base case (Table 3). The diurnal cycles in the WRF sensitivity simulations (Figure S2) have higher night-time NOx and lower night-time O_3 compared to the base case. Ground-level ozone at night is removed by reaction with NO (to form NO_2) and deposition, and can be replenished from higher-layer ozone. Night-time concentrations of NOx and O_3 were sensitive to the minimum vertical diffusion coefficient (K_v, set to 0.04 m^2/s or 0.1 m^2/s) but were not systematically better in either sensitivity test.

SO_2 performance shows positive bias at most coastal stations while the modeled and observed concentrations are in a fairly good agreement inland suggesting that contributions from ship emissions to surface SO_2 might be over-estimated. A likely reason for SO_2 overestimation at coastal locations is that all ship emissions were placed in the first model layer. As discussed above, many large vessels have sufficient stack height to release emissions into the second model layer. However, model results were insensitive to using an alternate vertical distribution of shipping emissions. This result may be due to limitations in the sensitivity test which could only move shipping emissions into the second layer for grid cells over open water. Model performance also was relatively insensitive to changing the vertical distribution of fire emissions because both vertical distributions placed most of the fire emissions within the planetary boundary layer.

Reducing biogenic isoprene emissions has small impacts to model performance in July, and the impacts mainly occur in the southern European countries (e.g., Italy and Spain). January model performance is insensitive to this change which is expected because of low biogenic emissions during winter.

Model results are relatively sensitive to a deposition scheme chosen. The Wesely/Slinn dry deposition model tends to generate higher ozone deposition rates than the Zhang model in summer, which overall leads to lower surface ozone concentrations. This effect is observed in our July results, but only resulted in 2-3% change in bias. In contrast, the Wesely/Slinn scheme increases winter ozone and improves FB by 11%. The deposition algorithms for aerosols in the two schemes have similar formulations, but parameterizations used in the Zhang scheme result in higher deposition velocity for

sub-micron aerosols, especially over rough vegetated surface. The Wesely/Slinn scheme improves the FB of PM_{10} from -59% to -43% in summer and from -47% to -12% in winter.

CB6 gas-phase chemistry improves January O_3 and PM performances considerably by increasing surface concentrations. January O_3 has 37% FB low bias compared to 63% in the base case. July O_3 and PM predictions also increase. Inorganic species, such as CO and SO_2, are also affected because of changes in oxidant availability. Although PM_{10} performance improves, it is still greatly under-estimated. Figure S3 shows that $PM_{2.5}$ performance is fairly good, especially in July, suggesting that the poor PM_{10} performance is primarily due to under-estimation of coarse material mass which suggests emission inventory problems. Analysis of PM_{10} and speciated components of PM using EMEP data (Figure S4) confirms that CAMx could not reproduce PM_{10} episodes, showing a mean low bias of 13.0 $\mu g/m^3$ in January at rural EMEP stations. The combined inorganic PM species (i.e. PSO_4, PNO_3, PNH_4) measured are generally less than 5 μg/m3 (compared to 20-40 $\mu g/m^3$ of PM_{10}) and the model could reproduce most of the mass, especially for PNO_3. The analysis suggests that emissions of coarse PM were underestimated.

Different inputs and assumptions affect model performance to different extents and depending upon pollutant. BCs and meteorology appear to impact overall model performance the most. MOZART compared to GEOS-Chem BCs give slightly better performance for pollutants affected by long-range transport, i.e., O_3 and CO. In constructing a new base case simulation for emission sensitivity analysis, two model configurations with combinations of changes were selected and tested. The first configuration (combo1) incorporates changes in vertical distributions of fire and ship emissions, and MOZART BCs. While changes to fire and ship emissions have insignificant impacts to model performance, the changes are considered appropriate thus included. The second configuration (combo2), in addition to the changes made in combo1, adds changes to biogenic isoprene emissions and CB6 chemistry. The MPE results for these two configurations are presented in Table 3 and Table S3. The performances vary by pollutant and by season. Both configurations improve ozone performances in January considerably because of the MOZART BCs while the combo2 predicts higher ozone due to CB6.

4. HDDM Sensitivity Analysis

The traditional approach to sensitivity analysis may be called the brute force method (BFM) where model simulations are repeated with different model inputs (as demonstrated earlier). While the BFM is easy to apply and interpretation of the result is straightforward, the method is computationally

demanding and susceptible to numerical uncertainty for small perturbations. The Decoupled Direct Method (DDM) offers an alternative to the traditional BFM by directly solving sensitivity equations derived from the governing equations of the model (Dunker, 1984; Dunker et al., 2002). The higher-order DDM (HDDM) adds the capability in CAMx for second order sensitivity coefficients which is used to understand non-linear responses and interactions between first-order sensitivities (Hakami et al., 2003; Koo et al., 2007).

In this work, HDDM was applied to the combo1 and combo2 scenarios for a 15-day July episode (July 16-28 with two spin-up days) selected because high ozone occurred in several major cities. First- and second-order ozone sensitivities were computed to domain-wide anthropogenic NOx and VOC emissions. The analysis focuses on the combo1 scenario because the results of combo2 are similar to those of combo1. Figure 1 shows episode average hourly ozone concentrations and the zero-out contributions (ZOC) of domain-wide anthropogenic NOx and VOC emissions at 11:00 GMT which corresponds to noon in British Summer Time (London) or 1 PM in Central European Summer Time (Milano). The ZOC of an emission source is defined as the amount by which concentrations would be reduced if that source was completely removed. Model response of concentrations to perturbations in input parameters can be approximated using Taylor series expansions:

$$C - C_0 = p_i S_i^{(1)} + p_j S_j^{(1)} + \tfrac{1}{2} p_i^2 S_i^{(2)} + \tfrac{1}{2} p_j^2 S_j^{(2)} + p_i p_j S_{ij}^{(2)} \quad (1)$$

$$S_i^{(1)} = \left.\frac{\partial C}{\partial p_i}\right|_{p_i=0}$$

$$S_{ij}^{(2)} = \left.\frac{\partial^2 C}{\partial p_i \partial p_j}\right|_{p_i=0;\, p_j=0}$$

where $C - C_0$ represents the concentration change due to simultaneous perturbation in two input parameters (i and j) by fractions p_i and p_j. Then, ZOC is calculated as follows:

$$ZOC(NOx) = C_0 - C(p_{NOx} = -100\%;\ p_{VOC} = 0) = S_{NOx}^{(1)} - \tfrac{1}{2} S_{NOx}^{(2)} \quad (2)$$

$$ZOC(VOC) = C_0 - C(p_{VOC} = -100\%;\ p_{NOx} = 0) = S_{VOC}^{(1)} - \tfrac{1}{2} S_{VOC}^{(2)} \quad (3)$$

In central and southern Europe, anthropogenic NOx contributions to O_3 are much higher than anthropogenic VOC contributions indicating that O_3 formation is mostly NOx-limited. This is primarily due to abundant biogenic VOC emissions in the region (Figure S5). Figure 2 decomposes

the source contributions of domain-wide anthropogenic NOx and VOC emissions to daily maximum ozone concentrations in the grid cells corresponding to London, Paris, Barcelona, Athens and Milano. All the sites generally show positive contributions of anthropogenic NOx and VOC with ZOC(NOx) greater than ZOC(VOC). Contributions of cross sensitivity are mostly negative meaning that ozone sensitivity to NOx emissions decreases as VOC emissions are reduced and vice versa. The source contributions do not sum to the modeled ozone concentrations because biogenic emissions, boundary conditions, fires, and higher-order nonlinear interactions also play a role. Contributions from these other sources account for significant portions of ozone concentrations at Athens and Barcelona.

London exhibits large day-to-day variations in the source contributions (e.g., anthropogenic NOx emissions negatively contribute daily maximum ozone concentration at London on July 24). Figure 3 shows ozone isopleths plots, which are constructed using Eq. (1), for daily maximum ozone concentrations at London on July 24 and 26. The response surfaces show markedly different patterns between the two days. On July 24, ozone production at the site is clearly VOC-limited whereas July 26 is close to the ridge line dividing NOx-limited and VOC-limited conditions. Therefore, if actual NOx emissions were higher than reported in the inventory, it could result shifting from the NOx-limited regime to the VOC-limited regime. At Milano, contributions of anthropogenic NOx emissions are consistently positive and large, and the ozone isopleths for episode average daily maximum ozone clearly show NOx-limited condition (Figure S6). It would require significant increases (60% or larger) in anthropogenic NOx emissions to change chemical regime of ozone formation at Milano.

5. Conclusions

CAMx modelling for the EU domain was completed for 2006 using input data for emissions, meteorology and BCs developed by AQMEII. Model performance for January and July exhibited under-estimation trends for all pollutants both in winter and summer, except for SO_2. SO_2 generally had little bias although some over-estimation occurred at coastal locations and this was attributed to incorrect vertical distribution of emissions from marine vessels. Performance for NO_X and NO_2 was better in winter than summer. The tendency to under-predict daytime NOx and O_3 in summer may result from insufficient NOx emissions or overstated daytime dilution (e.g., too deep planetary boundary layer). Winter O_3 was biased low and this was attributed to a low-bias in the O_3 boundary conditions. PM_{10} was widely under-predicted in both winter and summer. The poor PM_{10} was influenced by under-estimation of coarse PM emissions.

The AQMEII approach to applying many models was to promote use of consistent data sources (e.g., emissions, BCs) and minimize uncertainties associated with use of differing inputs by each model. However, most models are using different meteorological data, several are using different BCs and a few are using different emissions. AQMEII is evaluating the ensemble of predictions from all models applied for Europe and may not be able to untangle the consequences of differing input data and assumptions. To investigate the influence of input data, assumptions and uncertainties on model performance for the EU domain, multiple simulations were conducted first to identify the role played by different input data. Alternate inputs and model configurations tested include BCs from alternate global models (GEOS-Chem and MOZART), meteorological conditions from WRF, reduced MEGAN isoprene emissions, modified vertical distributions for fire and shipping emissions, and alternate deposition (Wesely/Slinn) and chemistry (CB6) schemes. The results show that the underlying boundary conditions, emission inventory and metrological input data play a crucial role in the air quality model performance.

Sensitivity analysis using HDDM was conducted to evaluate ozone sensitivity (at second order) to domain-wide anthropogenic precursor emissions (NOx and VOC). The results suggest that ozone production over the central and southern Europe during summer is mostly NOx-limited. Combining the first- and second-order sensitivity coefficients enables construction of ozone isopleths which can be used to determine the robustness of the chemical regime of ozone formation (NOx-limited or VOC-limited) in a region. Cities in southern Europe were consistently NOx-limited but London changed between NOx-limited and VOC-limited from day to day.

Acknowledgement

This study was supported by Coordinating Research Council Atmospheric Impacts Committee.

References

Air Sciences, Inc., 2005. 2002 Fire Emission Inventory for the WRAP Region – Phase II, Prepared for the Western Governors Association/WRAP by Air Sciences, Inc., Denver, CO.

Appel, W., R.C. Gilliam, N. Davis, A. Zubrow, S.C. Howard, 2010. Overview of the atmospheric model evaluation tool (AMET) v1.1 for evaluating meteorological and air quality models. Environmental Modelling & Software, 26: 434-443.

de Leeuw, G, Neele, F.P., Hill, M., Smith, M.H., Vignati, E., 2000. Production of sea spray aerosol in the surf zone. J. Geophys. Res. 105: 29,397-29,409.

Chemel, C., 2010. Personal communication.

Denier van der Gon, H., 2010. Personal communication to AQMEII project participants.

Dunker, A.M., 1984. The decoupled direct method for calculating sensitivity coefficients in chemical kinetics. Journal of Chemical Physics, 81 (5), 2385-2393.

Dunker, A.M., Yarwood, G., Ortmann, J.P., Wilson, G.M., 2002. The decoupled direct method for sensitivity analysis in a three-dimensional air quality model – Implementation, accuracy, and efficiency. Environmental Science & Technology, 36 (13), 2965-2976.

Emmons, L. K., Walters, S., Hess, P. G., Lamarque, J.-F., Pfister, G. G., Fillmore, D., Granier, C., Guenther, A., Kinnison, D., Laepple, T., Orlando, J., Tie, X., Tyndall, G., Wiedinmyer, C., Baughcum, S. L., Kloster, S., 2010. Description and evaluation of the Model for Ozone and Related chemical Tracers, version 4 (MOZART-4), Geosci. Model Dev., 3, 43-67, doi:10.5194/gmd-3-43-2010.

ENVIRON, 2010 . User's Guide to the Comprehensive Air Quality Model with Extensions (CAMx). Version 5.2.Available at: http://www.camx.com.

European Environment Agency, 2010. AirBase - The European air quality database. Available at: http://www.eea.europa.eu/data-and-maps/data/airbase-the-european-air-quality-database.

European Monitoring and Evaluation Program, 2010. EMEP particulate matter data. Available at: http://tarantula.nilu.no/projects/ccc/emepdata.html.

Gong, S. L., 2003. A parameterization of sea-salt aerosol source function for sub- and super-micron particles. Global Biogeochemical Cycles **17**: 1097-1104.

Galmarini, S., R. Bianconi, R. Addis, S. Andronopoulos, 2004. Ensemble dispersion forecasting – Part II: application and evaluation. Atmospheric Environment, 38:4619-4632.

Guenther, A., Karl, T., Harley, P.,Wiedinmyer, C., Palmer, Geron, C., 2006. Estimates of global terrestrial isoprene emissions using MEGAN (Model of Emissions of Gases and Aerosols from Nature), Atmos. Chem Phys., 6, 3181-3210.

Hakami, A., Odman, M.T., Russell, A.G., 2003. High-order, direct sensitivity analysis of multidimensional air quality models. Environmental Science & Technology, 37 (11), 2442-2452.

Koo, B., Yarwood, G., Cohan, D.S., 2007. Incorporation of High-order Decoupled Direct Method (HDDM) Sensitivity Analysis Capability into CAMx, Prepared for Texas Commission on Environmental Quality.

Mollner, A.K., Valluvadasan, S., Feng, L., Sprague, M.K., Okumura, M., Milligan, D.B., Bloss, W.J., Sander, S.P. , Martien, P.T. , Harley, R.A., McCoy, A.B., Carter, W.P.L., 2010. Rate of Gas Phase Association of Hydroxyl Radical and Nitrogen Dioxide, Sci., 330, 646.

Passant, N.R., 2002. Speciation of UK emissions of non-methane volatile organic compounds. AEA Technology Report ENV-0545, Culham, Abingdon, United Kingdom.

Pouliot, G. 2008. A Tale of Two Models: A Comparison of the Biogenic Emission Inventory System (BEIS3.14) and the Model of Emissions of Gases and Aerosols from Nature (MEGAN 2.04). Presented at 7th Annual CMAS Conference, Chapel Hill, NC, 6-8 October.

Sakulyanontvittaya, T., Duhl, T., Wiedinmyer, C., Helmig, D., Matsunaga, S., Potosnak, M., Milford, J., Guenther, A., 2008. Monoterpene and Sesquiterpene Emission Estimates for the United States, Environ. Sci. Technol., 42: 1623-1629.

Schere, K., 2010. Trace Gas/Aerosol Boundary Concentrations for AQMEII, presented at the second AQMEII workshop, Torino, Italy, 26 September 2010.

Slinn, S.A., Slinn. W.G.N., 1980. Predictions for particle deposition on natural waters. Atmos. Environ., **24**, 1013-1016.

Smith, M.H., Harrison, N. M., 1998. The Sea Spray Generation Function. Journal of Aerosol Science 29(Suppl I): S189-S190.

Sofiev, M., Hakkarainen, J., Vankevich R., 2010. European fire emission data for 2006 for the AQMEII simulations. presented at the second AQMEII workshop, Torino, Italy, 26 September 2010.

Starcrest Consulting Group, LLC., 2004. Port-Wide Baseline Air Emissions Inventory. Prepared for the Port of Los Angeles, California.

UCAR, 2010. MOZART-4 Results. Data located at: < http://www.acd.ucar.edu/wrf-chem/mozart.shtml> accessed on December 2010.

Vautard, R., 2010. Personal communication to AQMEII project participants.

Visschedijk, A. J. H., Zandveld, P., and Denier van der Gon, H. A. C., 2007. A high resolution gridded European emission database for the EU integrated project GEMS, TNO, Apeldoorn, Netherlands, TNO-report 2007-A-R0233/B.

Warneke, C., De Gouw, J.A., Del Negro, L., Brioude, J., McKeen, S., Stark, H., Kuster, W.C., Goldan, P.D., Trainer, M., Fehsenfeld, F.C., Wiedinmyer, C., Guenther, A.B., Hansel, A., Wisthaler, A., Atlas, E., Holloway, J.S., Ryerson, T.B., Peischl, J., Huey L.G., Case Hanks, A.T., 2010. Biogenic emission measurement and inventories determination of biogenic emissions in the eastern United States and Texas and comparison with biogenic emission inventories, J. Geophys. Res., 115, p. 21,doi:10.1029/2009JD012445.

Wesely, M.L., 1989. Parameterization of Surface Resistances to Gaseous Dry Deposition in Regional-Scale Numerical Models. Atmos. Environ., 23, 1293-1304.

Yantosca, B., Carouge, C., 2010. GEOS–Chem v8–03–01 Online User's Guide. http://acmg.seas.harvard.edu/geos/doc/man/

Yarwood, G., Rao, S., Yocke, M., Whitten, G., 2005. Updates to the Carbon Bond Chemical mechanism: CB05, report, Rpt. RT-0400675, US EPA, Res. Tri. Park.

Yarwood, G., Whitten, G.Z., Jung, J., 2010. Development, Evaluation and Testing of Version 6 of the Carbon Bond Chemical Mechanism (CB6), Final Report prepared for Texas Commission on Environmental Quality, September.

Zhang, L., Gong, S., Padro, J., Barrie., L., 2001. A size-segregated particle dry deposition scheme for an atmospheric aerosol module. Atmos. Environ., **35**, 549-560.

Zhang, L., Brook, J. R., Vet., R., 2003. A revised parameterization for gaseous dry deposition in air-quality models. Atmos. Chem. Phys., **3**, 2067–2082.

Table 1. Anthropogenic emissions by SNAP sector for 2006 (metric tons/year)

	SNAP Sector	CO	NOx	NMVOC	CH4	NH3	SO2	PM10
1	Combustion in energy industries	762,912	2,903,396	120,552	774,388	5,984	7,781,377	431,632
2	Non-industrial combustion	11,340,097	833,530	1,137,160	677,509	10,978	791,519	866,201
3	Combustion in manufacturing Industry	4,003,572	1,849,805	177,135	278,575	5,854	1,900,364	313,757
4	Production processes	3,282,061	378,349	1,082,172	61,159	120,157	492,550	535,376
5	Energy extraction and distribution	149,083	41,399	941,238	5,595,385	930	239,703	66,655
6	Solvent use	27,422	184	4,495,530	0	9,760	6,766	59,816
7	Road transport	14,262,267	5,085,578	2,635,363	113,785	81,671	90,220	402,004
8	Other mobile sources	3,288,189	5,408,350	756,676	6,159	3,048	2,563,899	496,021
9	Waste treatment and disposal	1,582,985	30,175	118,913	8,609,183	121,147	7,753	102,764
10	Agriculture	190,261	193,548	538,112	12,749,030	4,889,872	3,173	412,733
	Total	38,888,849	16,724,314	12,002,851	28,865,173	5,249,401	13,877,324	3,686,959

Table 2. Definitions of statistical metrics of model performance

Metric (potential range)	Definition
Normalized Mean Bias (-100% to +∞)	$NMB = \frac{\sum_{i=1}^{N}(C_m - C_o)}{\sum_{i=1}^{N} C_o}$
Normalized Mean Error (0% to +∞)	$NME = \frac{\sum_{i=1}^{N}\lvert C_m - C_o\rvert}{\sum_{i=1}^{N} C_o}$
Fractional Bias (-200% to +200%)	$FB = \frac{1}{N}\sum_{i=1}^{N}\frac{(C_m - C_o)}{\left(\frac{C_o + C_m}{2}\right)}$
Fractional Error (0% to +200%)	$FE = \frac{1}{N}\sum_{i=1}^{N}\frac{\lvert C_m - C_o\rvert}{\left(\frac{C_o + C_m}{2}\right)}$

C_o = observation
C_m = model prediction
N = number of data pairs (C_o, C_m)

Table 3. Statistical metrics[1] of model performance for January and July 2006

Sensitivity Case[2]	January MPE				July MPE				January MPE				July MPE			
	NMB	NME	FB	FE	NMB	NME	FB	FE	NMB	NME	FB	FE	NMB	NME	FB	FE
	O_3								NOx							
Base Case	-48	50	-63	70	-4.0	16	-1.9	20	-37	47	-51	74	-51	54	-75	83
BC_MOZART	3.5	34	0.2	41	4.2	16	6.3	20	-44	49	-63	80	-52	54	-77	84
BC_GEOS	-19	34	-21	44	0.3	16	2.6	20	-40	48	-58	77	-52	54	-76	84
WRF_0p1	-72	73	-110	115	-15	28	-21	40	-8.3	55	-13	70	-3.1	51	-3.2	61
WRF_0p04	-80	80	-131	134	-21	32	-29	45	8.5	65	5.5	71	5.8	53	7.0	62
Bio	-48	50	-63	70	-6.4	16	-4.8	21	-37	47	-51	74	-50	53	-74	83
Fire	-48	50	-63	70	-4.0	16	-1.9	20	-37	47	-51	74	-51	54	-75	83
Ship	-48	50	-62	70	-3.7	16	-1.6	20	-37	47	-52	74	-52	54	-77	84
Deposition	-43	46	-54	63	-6.3	16	-4.5	21	-30	47	-41	71	-47	51	-68	78
Chem_CB6	-32	40	-37	54	7.2	16	9.4	21	-39	48	-56	77	-50	53	-74	82
Combo1	4.0	35	0.6	41	4.5	16	6.6	20	-44	50	-64	80	-53	54	-78	85
Combo2	25	40	19	42	14	19	15	22	-46	51	-68	83	-52	53	-76	84
	NO_2								CO							
Base Case	-38	40	-48	61	-46	49	-62	73	-37	42	-45	63	-13	33	-11	44
BC_MOZART	-35	38	-48	62	-46	50	-63	74	-35	41	-43	62	-18	34	-17	47
BC_GEOS	-35	38	-46	60	-46	50	-62	73	-36	42	-45	62	-24	36	-24	50
WRF_0p1	-27	35	-29	53	-0.1	45	-0.3	54	-17	41	-20	57	64	76	48	62
WRF_0p04	-25	35	-25	52	8.5	46	8.5	53	-4.5	44	-7.1	56	91	99	61	71
Bio	-38	40	-48	61	-45	49	-61	72	-37	42	-45	63	-15	33	-14	45
Fire	-38	40	-48	61	-46	49	-62	73	-37	42	-45	63	-12	33	-10	44
Ship	-38	40	-49	61	-47	50	-63	74	-37	42	-46	63	-13	33	-11	44
Deposition	-23	33	-30	53	-41	46	-53	68	-37	42	-45	63	-12	33	-11	44
Chem_CB6	-35	38	-46	60	-45	49	-60	72	-38	43	-47	64	-25	35	-26	50
Combo1	-35	39	-49	62	-47	50	-64	74	-35	41	-43	62	-17	34	-16	47
Combo2	-34	38	-49	63	-46	49	-62	73	-37	42	-45	62	-30	38	-33	53
	SO_2								PM_{10}							
Base Case	1.1	61	0.4	68	9.1	60	6.9	64	-38	51	-47	73	-44	46	-59	64
BC_MOZART	2.3	61	1.8	68	8.6	60	6.5	64	-33	52	-39	71	-49	51	-68	72
BC_GEOS	3.2	62	3.0	68	10	60	7.7	64	-35	53	-42	73	-52	53	-72	76
WRF_0p1	-5.3	64	-5.8	71	42	85	31	72	-34	53	-42	73	-21	35	-23	48
WRF_0p04	-5.3	66	-6.2	73	41	87	31	73	-34	54	-41	74	-18	35	-19	47
Bio	1.2	61	0.4	68	8.9	60	6.9	64	-38	51	-47	73	-44	46	-59	65
Fire	1.2	61	0.4	68	9.2	60	7.1	64	-38	51	-47	73	-43	45	-58	64
Ship	1.0	61	0.1	68	9.1	60	6.8	64	-38	51	-47	73	-44	46	-59	64
Deposition	5.7	64	4.5	69	8.6	59	6.5	64	-9.0	56	-12	65	-34	38	-43	52
Chem_CB6	14	68	12	70	20	65	15	65	-28	52	-33	69	-38	41	-50	57
Combo1	2.0	61	1.5	68	8.7	60	6.4	64	-33	52	-39	71	-48	50	-66	71
Combo2	15	68	14	69	18	64	14	64	-23	54	-26	68	-43	45	-57	63

[1]See Table 2 for definitions of the statistical metrics.

[2]BC_MOZART = replacing GEMS BCs with MOZART BCs; BC_GEOS = replacing GEMS BCs with GEOS-Chem BCs; WRF_0p1 = replacing MM5 with WRF using minimum Kv of 0.1; WRF_0p04 = similar to WRF_0p1 but with minimum Kv of 0.04; Bio = decreasing biogenic isoprene emissions by half; Fire = reducing vertical plume heights of fire emissions; Ship = placing 75% of shipping emissions into 2nd model layer; Deposition = using Wesely/Slinn dry deposition scheme; Chem_CB6 = using CB6 gas-phase chemistry; Combo1 = BC_MOZART+Fire+Ship; Combo2 = Combo1+Bio+CB6.

(a) O3 at 11:00 GMT

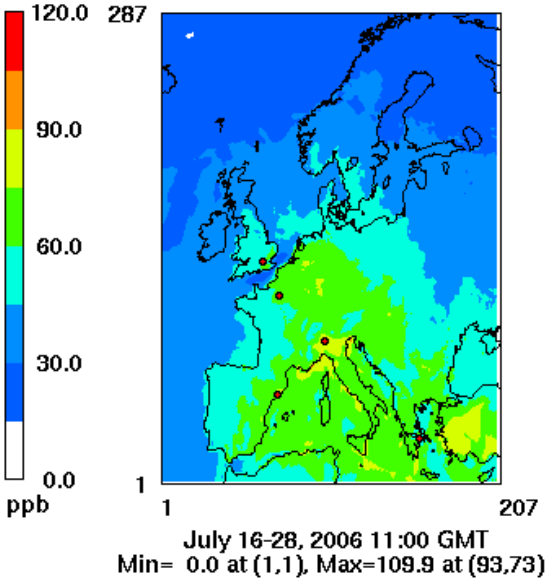

(b) ZOC(NOx) at 11:00 GMT

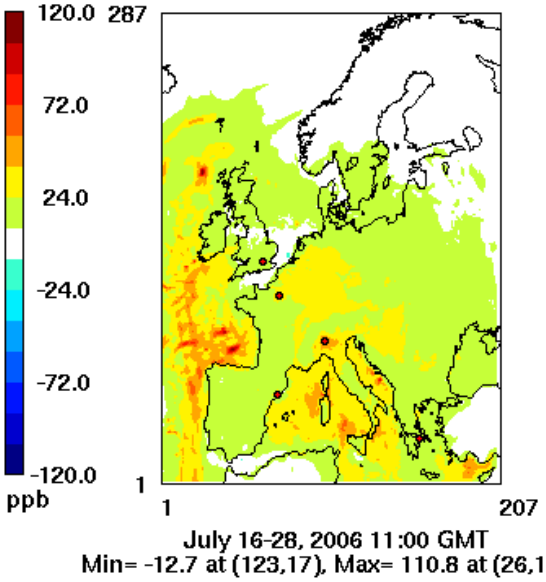

(c) ZOC(VOC) at 11:00 GMT

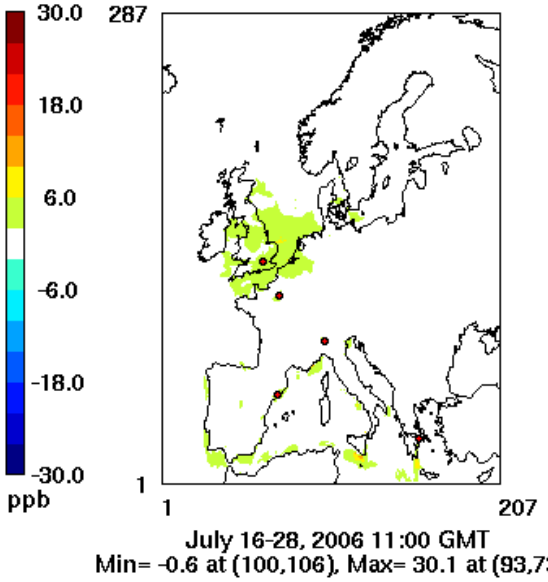

Figure 1. Episode average hourly ozone concentrations and zero-out contributions (ZOC) estimated by HDDM at 11:00 GMT. ZOC(NOx) and ZOC(VOC) are computed by Eqs. (2) and (3), respectively. Red dots correspond to London, Paris, Milano, Barcelona, and Athens (from top to bottom).

(a) London

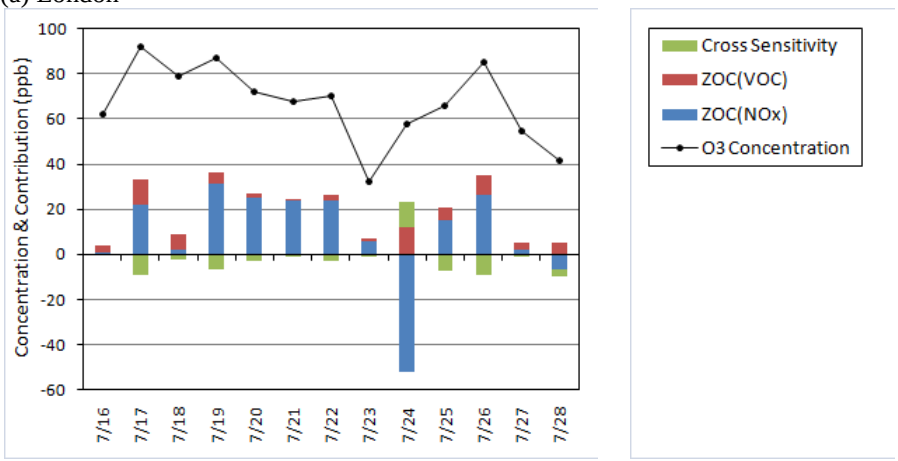

(b) Paris

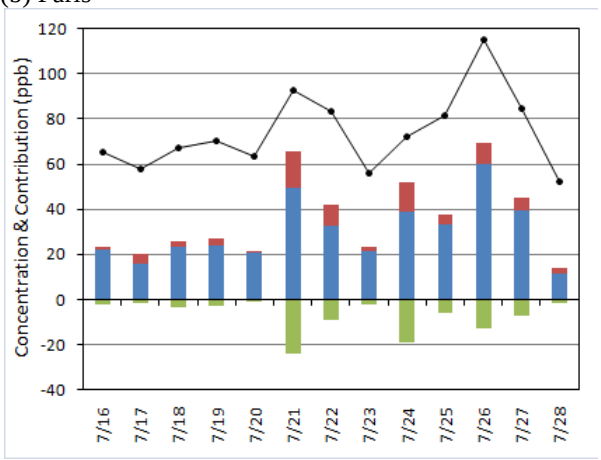

(c) Barcelona

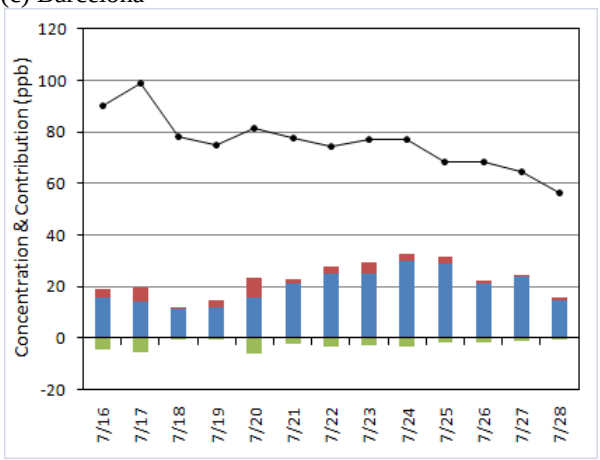

(d) Athens

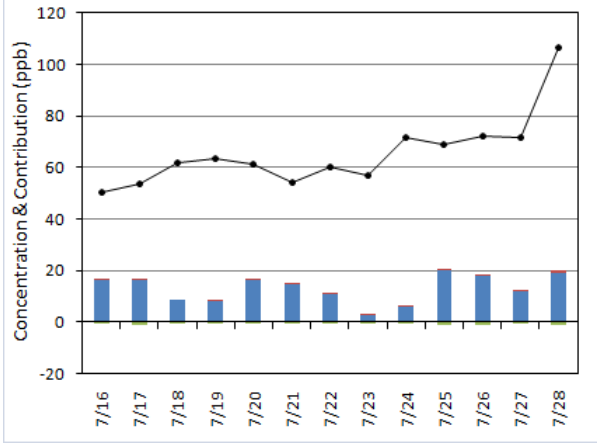

(e) Milano

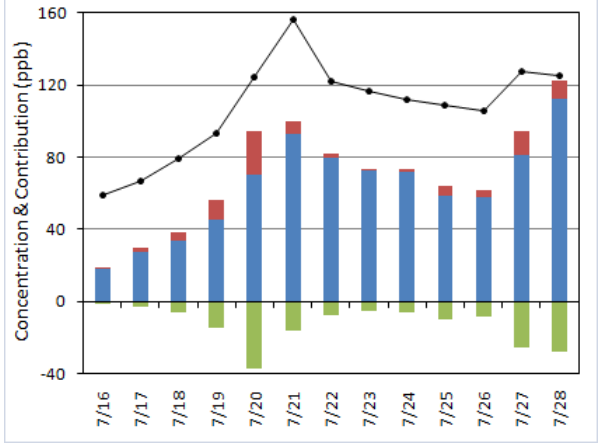

Figure 2. Daily maximum hourly ozone concentrations and zero-out source contributions estimated by HDDM at London, Paris, Barcelona, Athens, and Milano. ZOC(NOx) and ZOC(VOC) are computed by Eqs. (2) and (3), respectively. Contribution of cross sensitivity = $-S^{(2)}_{NOx,VOC}$.

(a) London (July 24, 13:00 GMT)

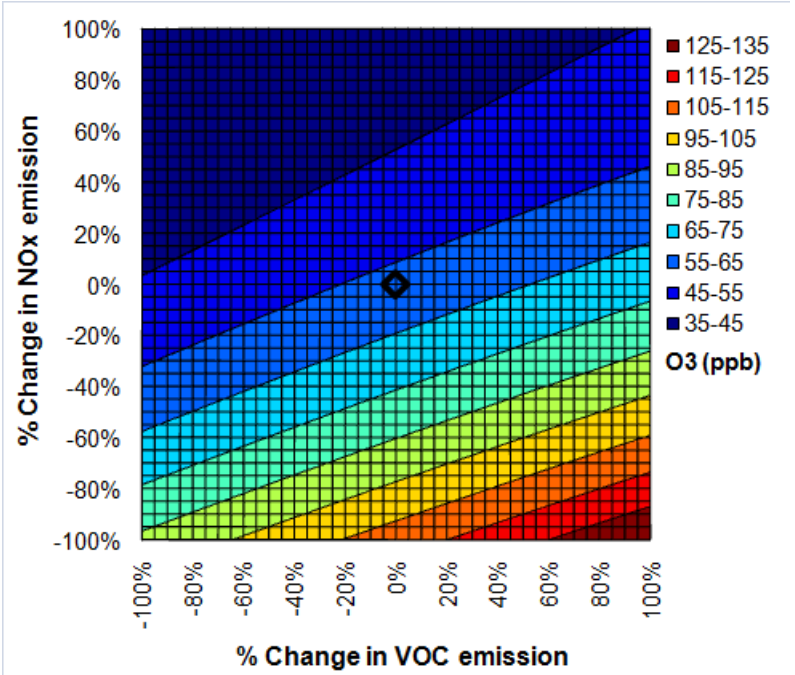

(b) London (July 26, 12:00 GMT)

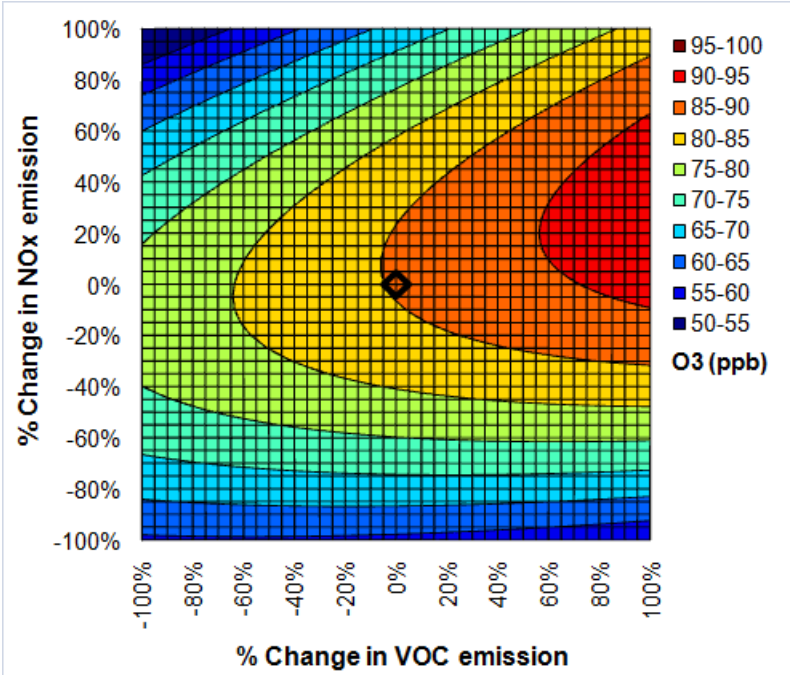

Figure 3. Ozone isopleths constructed using the first- and second-order sensitivity coefficients (Eq. (1)) at London (July 24, 13:00 GMT & July 26, 12:00 GMT).

Supplementary Information

Table S1. Anthropogenic emissions by country or sea area for 2006 (metric tons/year)

Country	CO	NOx	NMVOC	CH4	NH3	SO2	PM10
Albania	112,326	25,535	32,309	177,786	24,398	31,255	9,085
Atlantic Ocean	51,968	517,315	17,888	0	0	359,895	43,423
Austria	705,024	215,984	164,276	331,057	63,927	28,083	46,382
Baltic Sea	36,123	346,739	12,166	0	0	224,834	26,126
Belarus	530,830	160,124	189,010	748,068	138,689	77,009	35,701
Belgium	851,588	276,772	198,578	364,228	73,206	136,104	42,188
Bosnia and Herzegovina	181,765	52,278	47,835	157,609	17,266	423,640	43,167
Black Sea	7,829	74,664	2,690	0	0	53,663	6,235
Bulgaria	759,381	222,748	153,547	473,961	57,186	850,382	82,997
Croatia	311,951	66,388	90,236	151,310	44,861	57,534	23,450
Cyprus	40,862	17,309	13,960	47,266	5,245	12,108	2,811
Czech Republic	479,382	266,888	177,971	496,595	67,524	201,389	33,910
Denmark	611,562	186,621	113,448	265,148	88,460	24,857	40,752
Estonia	152,419	30,496	33,671	89,287	9,251	69,561	25,191
Finland	512,576	192,753	132,647	217,140	36,819	86,065	49,467
France	5,169,230	1,151,452	1,349,980	2,634,445	727,597	432,793	492,543
Germany	4,038,311	1,426,299	1,209,808	2,161,306	616,090	567,324	194,266
Greece	605,382	297,184	341,096	403,967	71,982	528,801	68,922
Hungary	579,742	205,224	177,069	365,692	80,164	429,133	53,681
Ireland	211,893	110,097	58,976	621,653	111,965	60,162	21,318
Italy	3,973,855	1,133,175	1,227,009	1,826,637	420,590	471,378	162,170
Latvia	329,923	42,812	65,278	81,543	14,082	11,139	15,290
Lithuania	195,033	60,016	80,253	162,992	34,854	40,426	21,253
Luxembourg	41,313	14,142	12,804	16,540	5,254	2,759	3,506
Malta	0	11,396	8,846	17,976	892	8,026	644
Mediterranean Sea	158,543	1,546,054	53,020	0	0	1,083,591	126,537
Moldavia	140,142	65,556	38,265	217,119	27,101	122,205	43,879
Moldova	103,700	39,368	25,814	90,380	7,340	103,569	18,668
Netherlands	587,992	325,026	169,808	773,771	131,972	51,193	38,851
North Sea	77,421	746,737	26,495	0	0	483,699	58,468
Norway	418,560	190,528	191,419	210,359	22,485	21,328	52,776
Poland	3,524,572	675,397	945,791	1,814,791	290,750	1,308,061	284,969
Protugal	601,561	250,065	285,711	519,955	69,912	192,286	45,949
Russia	1,442,338	347,498	319,504	2,170,613	88,484	427,290	187,464
Serbia	1,368,525	290,248	391,122	1,216,704	195,507	571,585	144,961
Slovakia	290,949	86,596	74,815	199,527	26,586	87,708	24,350
Slovenia	77,066	58,019	41,911	99,100	18,703	35,681	9,405
Spain	2,191,555	1,445,946	1,051,691	1,751,802	442,340	1,235,055	203,821
Sweden	573,083	201,452	191,128	262,253	51,646	39,180	52,663
Switzerland	318,258	83,363	104,143	166,429	55,130	16,276	19,331
Turkey	1,924,232	662,163	523,038	1,531,449	257,292	1,349,459	269,119
Ukraine	2,014,849	845,175	569,494	3,172,935	465,971	530,874	325,959
United Kingdom	2,289,536	1,601,490	943,601	2,321,972	316,584	688,957	151,998
Yugoslavia	313,851	165,492	147,141	529,754	67,740	358,676	84,075
Total	**38,907,001**	**16,730,584**	**12,005,262**	**28,861,119**	**5,245,845**	**13,894,993**	**3,687,721**

Table S2. Average daily emissions by source category in January and July 2006 (metric tons/day)

Source Category	CO	NOx	NMVOC	CH4	NH3	SO2	PM10
				January			
Anthropogenic	124,122	45,790	31,554	64,742	7,034	43,647	11,243
Biogenic	1,438	155	5,295	119	-	-	-
Fire	4,977	154	69	-	74	21	671
Sea Salt	-	-	-	-	-	-	65,148
Total	**130,537**	**46,099**	**36,918**	**64,861**	**7,108**	**43,668**	**77,062**
				July			
Anthropogenic	80,309	41,990	27,873	68,870	12,373	31,458	7,708
Biogenic	22,979	2,295	171,372	1,289	-	-	-
Fire	196,991	6,078	2,719	-	2,934	838	26,594
Sea Salt	-	-	-	-	-	-	15,917
Total	**300,279**	**50,363**	**201,964**	**70,159**	**15,307**	**32,296**	**50,219**

Table S3. Statistical metrics of model performance by monitor location type for January and July 2006

Sensitivity Case	Rural Stations								Urban Stations							
	January MPE				July MPE				January MPE				July MPE			
	NMB	NME	FB	FE	NMB	NME	FB	FE	NMB	NME	FB	FE	NMB	NME	FB	FE
					O_3								O_3			
Base Case	-52	53	-74	78	-9.3	17	-7.7	21	-44	47	-54	63	-1.3	16	0.5	20
BC_MOZART	-5.8	30	-10	40	-2.1	16	0.5	20	13	36	9.0	40	7.3	16	8.9	20
BC_GEOS	-26	33	-33	47	-5.5	16	-3.3	20	-11	33	-12	40	3.2	16	5.0	20
WRF_0p1	-71	72	-112	116	-23	30	-31	43	-71	72	-107	113	-13	28	-19	40
WRF_0p04	-80	80	-134	136	-31	35	-42	51	-78	79	-127	131	-19	31	-27	44
Bio	-52	53	-74	78	-12	18	-10	22	-44	47	-54	63	-3.6	16	-2.3	20
Fire	-52	53	-74	78	-9.3	17	-7.7	21	-44	47	-54	63	-1.2	16	0.5	20
Ship	-52	53	-74	78	-9.0	17	-7.4	21	-44	47	-54	63	-1.0	16	0.9	20
Deposition	-48	49	-65	70	-11	18	-10	22	-38	43	-46	57	-3.9	15	-2.1	20
Chem_CB6	-39	43	-50	60	0.9	15	3.4	19	-25	38	-29	48	10	17	12	21
Combo1	-5.6	30	-10	40	-1.8	16	0.8	20	14	37	9.4	40	7.6	16	9.3	20
Combo2	11	33	7.4	38	7.1	16	9.4	20	38	46	28	44	17	20	18	24
					NOx								NOx			
Base Case	5.3	48	-0.2	58	-31	42	-47	64	-48	51	-73	82	-60	61	-90	95
BC_MOZART	-6.2	43	-17	58	-33	42	-49	65	-54	55	-84	89	-61	61	-92	95
BC_GEOS	-1.3	44	-9.1	57	-32	42	-48	65	-51	53	-79	86	-61	61	-91	95
WRF_0p1	50	93	37	76	17	55	20	61	-23	50	-33	69	-16	50	-18	63
WRF_0p04	95	135	58	85	33	62	33	65	-9.1	53	-16	67	-9	52	-9.2	62
Bio	5.4	48	-0.2	58	-30	41	-45	64	-48	51	-73	82	-60	60	-90	94
Fire	5.4	48	-0.2	58	-31	42	-46	64	-48	51	-73	82	-60	61	-90	94
Ship	5.0	47	-0.8	58	-32	41	-49	64	-48	51	-74	82	-61	61	-92	95
Deposition	18	58	13	61	-24	39	-35	59	-42	47	-63	76	-57	58	-84	89
Chem_CB6	0.7	46	-6.0	58	-29	41	-45	63	-50	53	-77	85	-60	60	-89	93
Combo1	-6.7	42	-17	58	-34	42	-51	65	-54	56	-84	90	-61	62	-93	96
Combo2	-10	42	-22	60	-32	41	-48	64	-56	57	-88	93	-61	61	-92	95
					NO_2								NO_2			
Base Case	-8.1	34	-10	48	-23	39	-29	54	-45	45	-63	67	-54	55	-77	83
BC_MOZART	-8.5	35	-14	49	-24	40	-31	54	-43	43	-63	68	-55	56	-78	83
BC_GEOS	-7.4	35	-10	48	-23	40	-30	54	-43	43	-61	66	-55	56	-78	83
WRF_0p1	7.0	44	9.4	52	31	54	29	55	-35	37	-44	55	-15	43	-16	54
WRF_0p04	10	46	13	53	49	65	40	59	-33	36	-40	53	-7.4	42	-8.1	51
Bio	-8.1	34	-10	48	-22	39	-28	54	-45	45	-63	67	-54	55	-77	82
Fire	-8.1	34	-10	48	-23	39	-29	54	-45	45	-63	67	-54	55	-77	83
Ship	-8.6	34	-11	49	-24	39	-32	54	-45	45	-63	68	-55	56	-79	84
Deposition	10	40	10	50	-14	38	-18	50	-33	35	-46	56	-50	52	-70	77
Chem_CB6	-5.9	34	-9.3	48	-21	39	-27	53	-43	43	-61	66	-54	55	-76	82
Combo1	-9.0	35	-14	50	-25	39	-33	55	-43	44	-63	68	-55	56	-80	84
Combo2	-8.5	35	-16	51	-23	39	-31	54	-42	43	-64	70	-54	55	-78	83

Table S3. Statistical metrics of model performance by monitor location type for January and July 2006 (continued)

Sensitivity Case	Rural Stations								Urban Stations							
	January MPE				July MPE				January MPE				July MPE			
	NMB	NME	FB	FE	NMB	NME	FB	FE	NMB	NME	FB	FE	NMB	NME	FB	FE
					CO								**CO**			
Base Case	-10	31	-10	47	-1.1	29	4.9	41	-38	42	-48	63	-13	32	-12	43
BC_MOZART	-7.4	31	-7.1	46	-8.5	31	-1.8	42	-37	41	-46	62	-18	33	-18	45
BC_GEOS	-8.4	31	-8.8	47	-16	32	-10	44	-38	42	-47	63	-24	35	-25	48
WRF_0p1	13	46	13	51	74	85	56	65	-19	40	-23	57	65	74	49	61
WRF_0p04	34	59	29	57	106	114	70	76	-6.8	43	-10	55	91	97	61	70
Bio	-10	31	-10	47	-4.2	28	2.1	41	-38	42	-48	63	-15	32	-14	43
Fire	-10	31	-10	47	0.1	29	5.8	41	-38	42	-48	63	-12	32	-11	43
Ship	-10	31	-10	47	-1.1	29	4.7	40	-38	42	-48	64	-13	32	-12	43
Deposition	-10	31	-10	47	-0.6	29	5.2	41	-38	42	-48	63	-13	32	-11	43
Chem_CB6	-12	30	-12	47	-18	31	-11	44	-39	43	-50	64	-25	34	-26	48
Combo1	-7.6	31	-7.4	46	-8.5	31	-1.1	42	-37	41	-46	62	-18	33	-17	45
Combo2	-9.5	30	-9.3	46	-26	34	-19	47	-38	42	-48	63	-30	37	-33	52
					SO_2								**SO_2**			
Base Case	13	66	10	66	7.3	51	4.5	61	-5.5	60	-5.5	68	7.5	60	5.8	64
BC_MOZART	15	66	12	65	7.1	51	3.8	61	-4.9	60	-4.3	68	7.0	59	5.4	64
BC_GEOS	16	66	14	65	8.1	51	5.5	60	-3.8	60	-3.1	67	8.2	60	6.5	64
WRF_0p1	-7.3	60	-11	67	24	62	21	64	-7.6	64	-6.4	71	41	83	32	73
WRF_0p04	-11	61	-15	69	19	62	18	65	-6.5	66	-5.6	72	41	86	32	74
Bio	13	66	10	66	7.0	51	4.4	60	-5.5	60	-5.5	68	7.3	60	5.8	64
Fire	13	66	10	66	7.5	51	4.7	61	-5.5	60	-5.5	68	7.6	60	5.9	64
Ship	13	65	10	66	7.4	51	4.7	61	-6.0	60	-5.9	68	7.3	59	5.5	64
Deposition	20	72	15	69	7.0	51	4.4	61	-2.1	62	-2.1	69	6.9	59	5.3	64
Chem_CB6	33	79	24	70	18	57	15	62	5.7	66	5.5	68	16	64	13	65
Combo1	14	66	12	65	7.1	51	4.0	61	-5.2	60	-4.7	68	6.9	59	5.2	64
Combo2	35	80	27	69	17	56	14	62	7.1	65	6.7	68	15	63	12	64
					PM10								**PM10**			
Base Case	-31	51	-38	69	-41	43	-54	60	-42	52	-52	75	-47	48	-62	67
BC_MOZART	-25	53	-29	67	-47	49	-65	69	-38	52	-45	73	-52	53	-71	74
BC_GEOS	-28	54	-33	69	-50	51	-69	73	-40	53	-47	75	-54	55	-75	78
WRF_0p1	-32	54	-37	72	-21	35	-23	48	-37	54	-46	75	-24	36	-27	48
WRF_0p04	-32	56	-38	73	-19	36	-20	48	-37	55	-45	75	-21	35	-23	47
Bio	-31	51	-38	69	-41	43	-54	60	-42	52	-52	75	-47	48	-63	67
Fire	-31	51	-38	69	-40	43	-53	59	-42	52	-52	75	-46	47	-61	66
Ship	-31	51	-38	70	-41	43	-54	60	-43	52	-53	75	-47	48	-62	67
Deposition	3.2	56	2.5	61	-29	35	-36	47	-15	56	-19	66	-37	40	-47	55
Chem_CB6	-20	53	-23	65	-34	38	-44	53	-33	51	-39	70	-41	43	-54	60
Combo1	-25	53	-29	67	-47	48	-63	68	-38	52	-45	73	-51	52	-69	73
Combo2	-14	54	-15	64	-40	42	-52	60	-28	54	-33	70	-45	47	-60	66

(a) Base Case

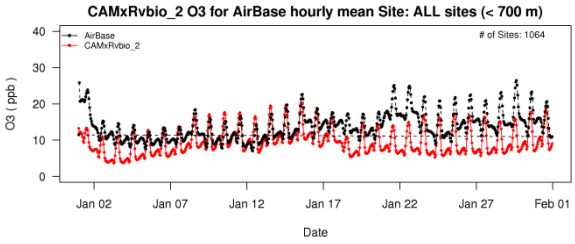

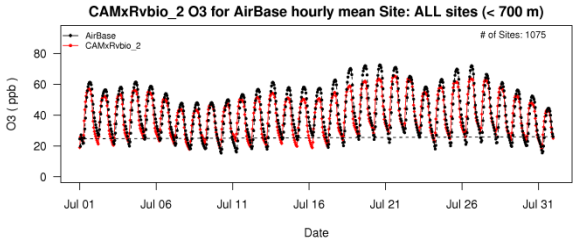

(b) BC_MOZART

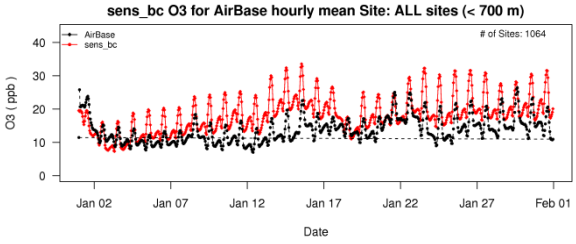

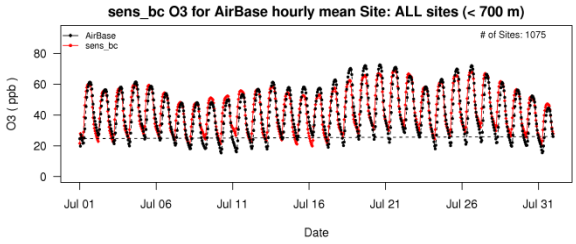

(c) BC_GEOS-CHEM

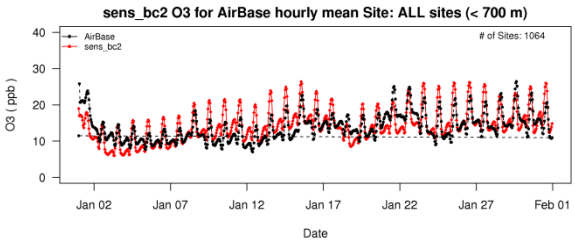

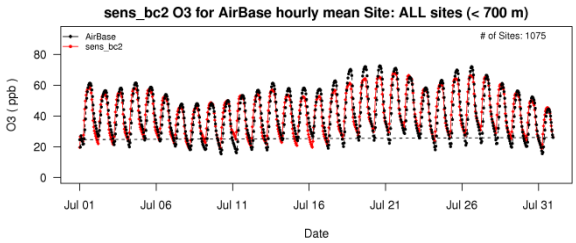

(d) Fire

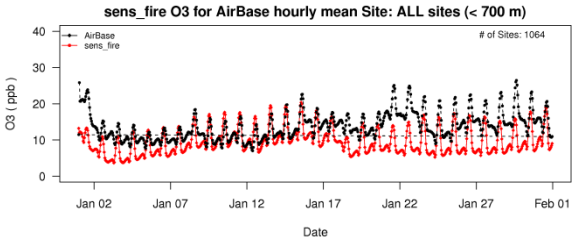

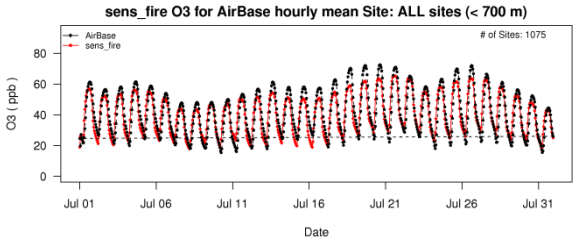

(e) Biogenic

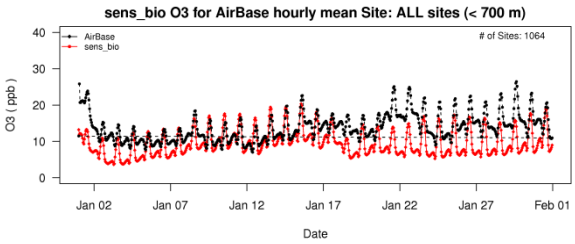

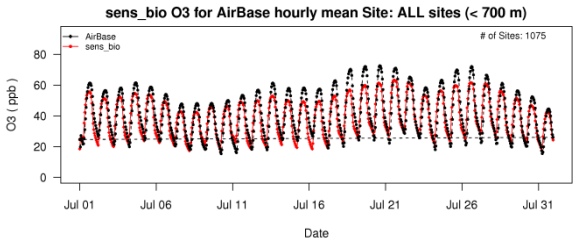

(f) WRF (Min(Kv) >= 0.1)

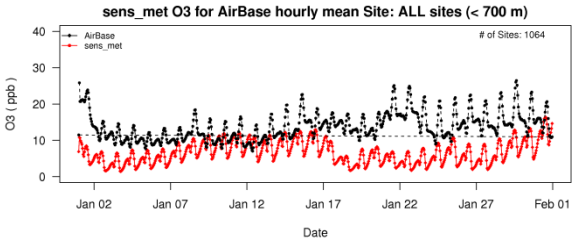

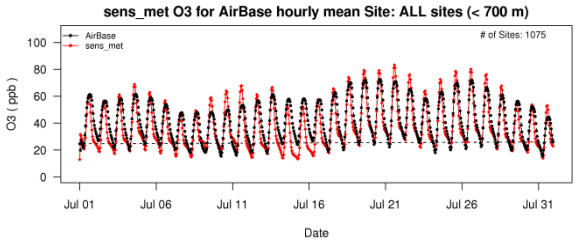

(g) WRF (Min(Kv) >= 0.04)

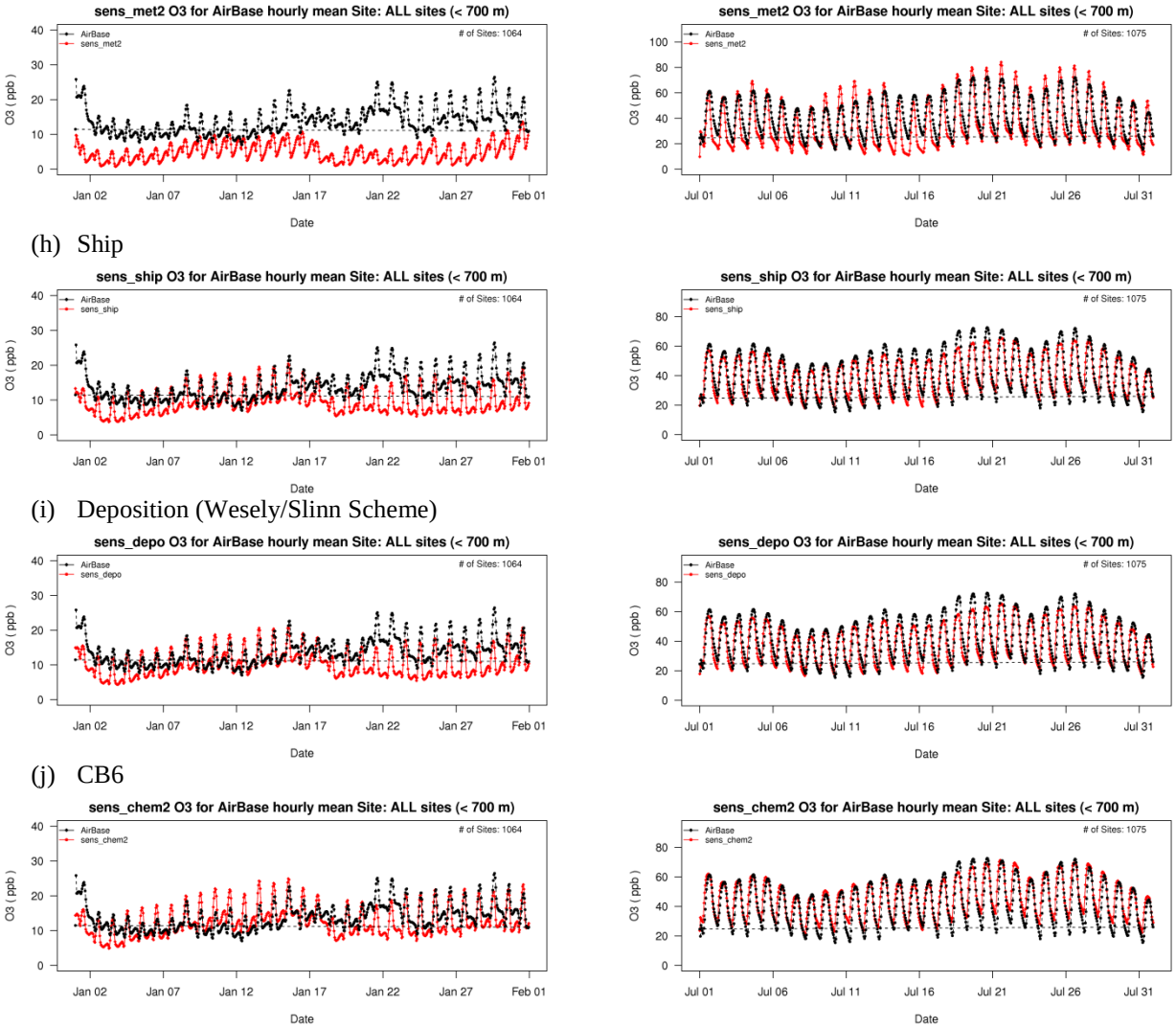

(h) Ship

(i) Deposition (Wesely/Slinn Scheme)

(j) CB6

Figure S1. Modeled and observed hourly concentrations of O_3 at 'All' AirBase stations for January (left) and July (right) 2006.

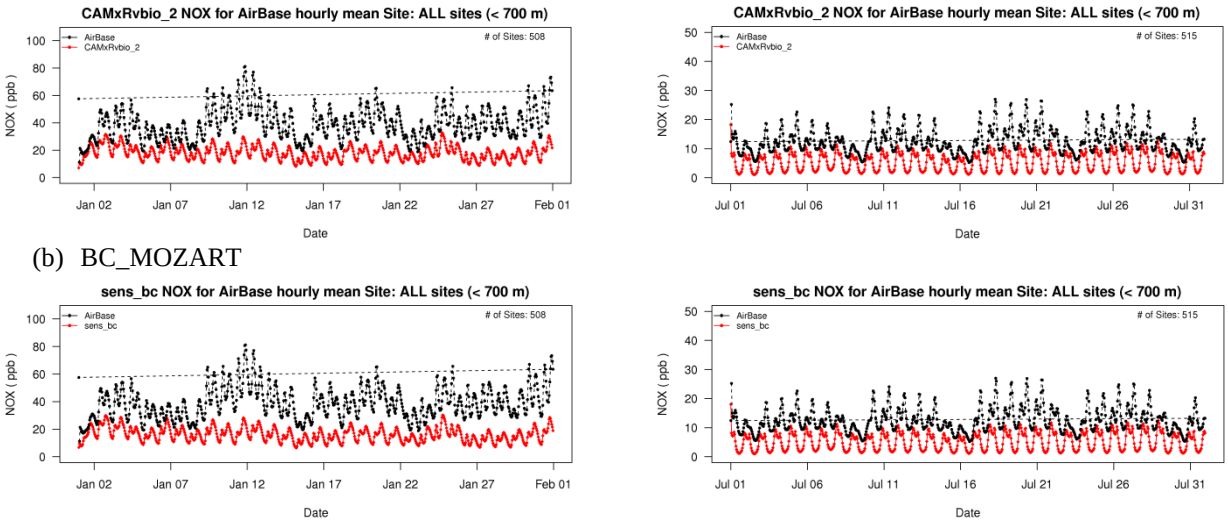

(a) Base Case

(b) BC_MOZART

(c) BC_GEOS-CHEM

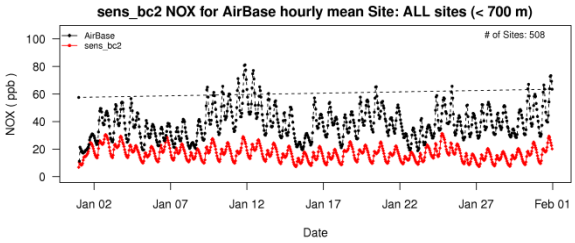

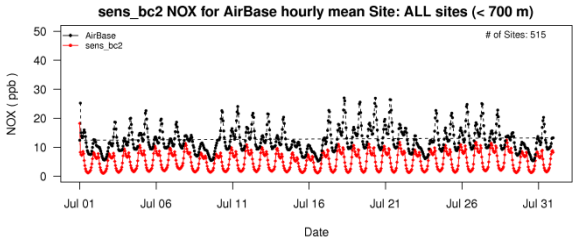

(d) Fire

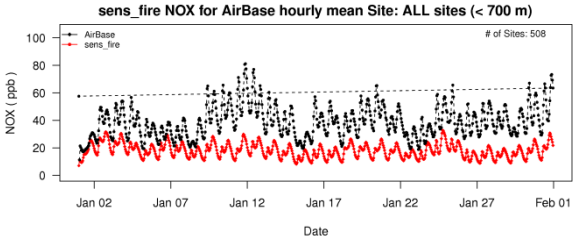

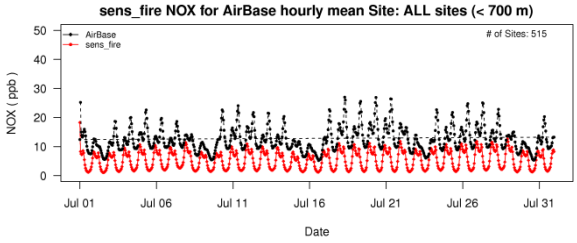

(e) Biogenic

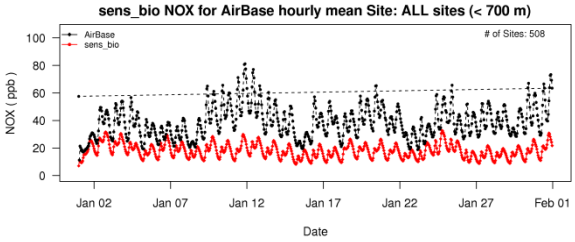

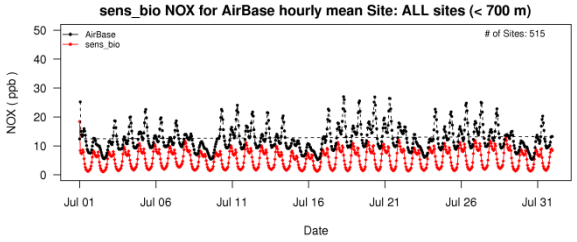

(f) WRF (Min(Kv) >= 0.1)

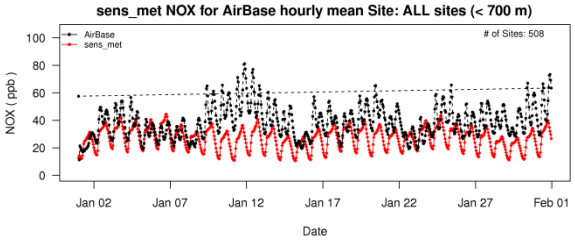

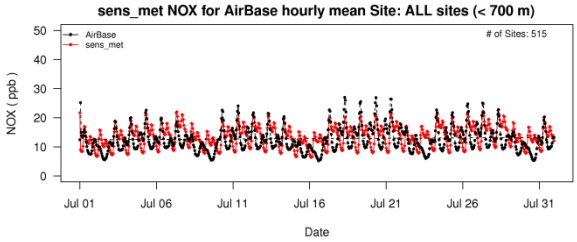

(g) WRF (Min(Kv) >= 0.04)

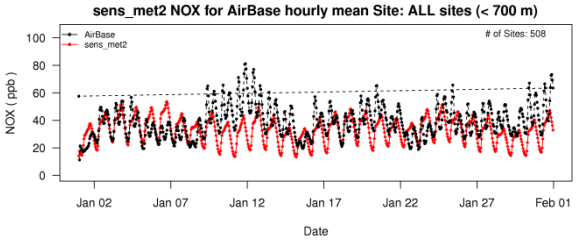

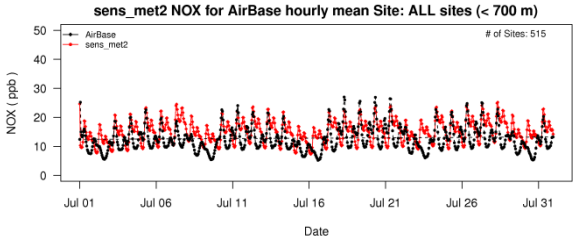

(h) Ship

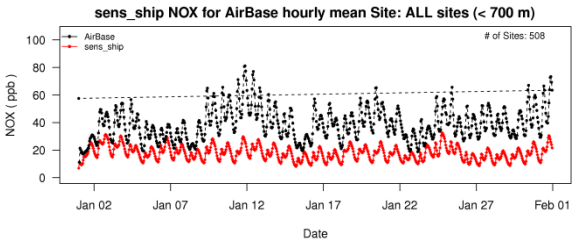

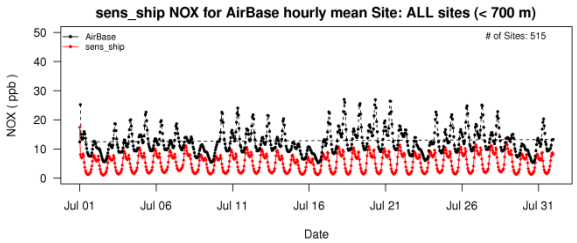

(i) Deposition (Wesely/Slinn Scheme)

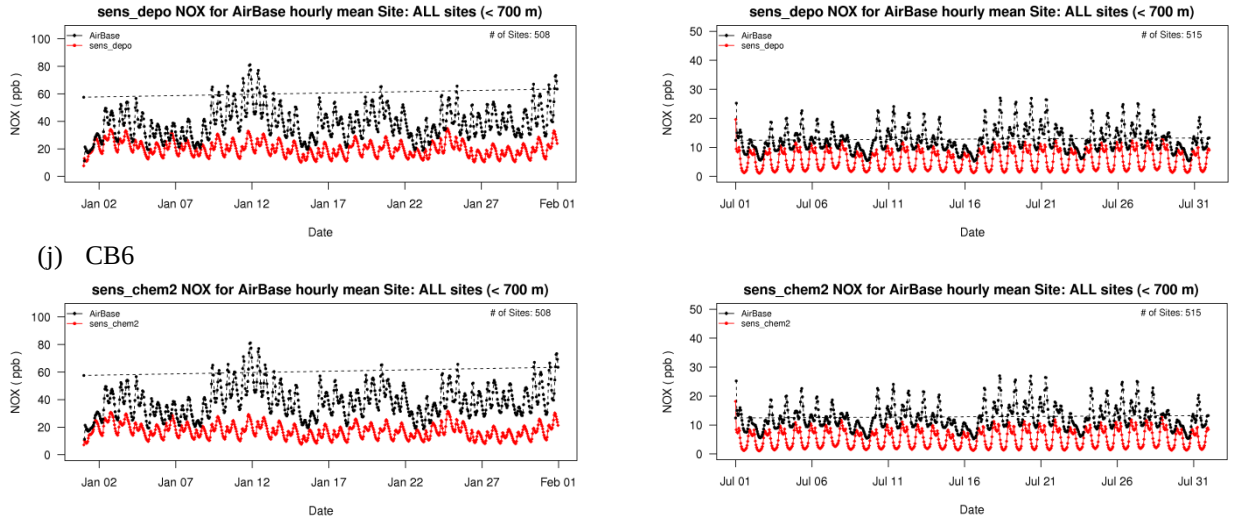

Figure S2. Modeled and observed hourly concentrations of NOx at 'All' AirBase stations for January (left) and July (right) 2006.

(a) PM_{10} (Base Case)

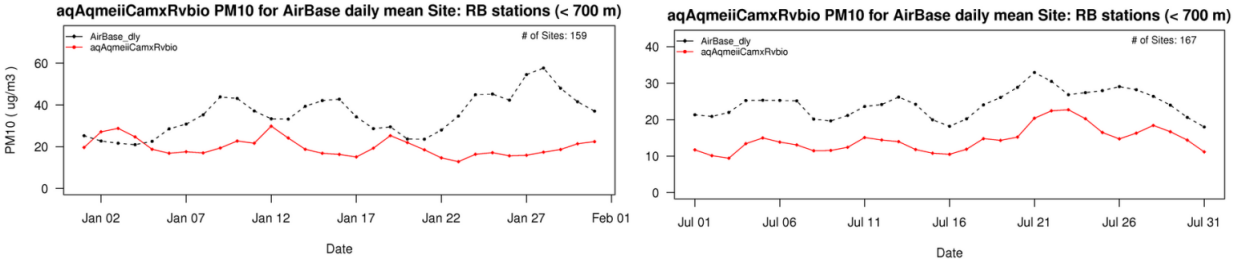

(b) $PM_{2.5}$ (Base Case)

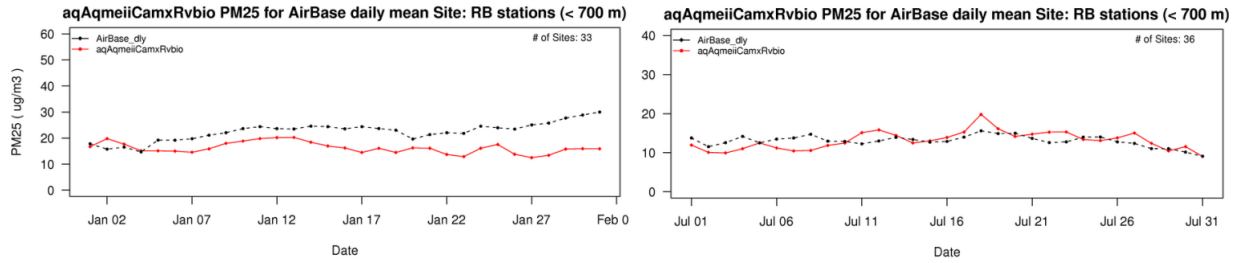

Figure S3. Modeled and observed daily mean concentrations of (a) PM_{10} and (b) $PM_{2.5}$ at AirBase rural background stations for January (left) and July (right) 2006.

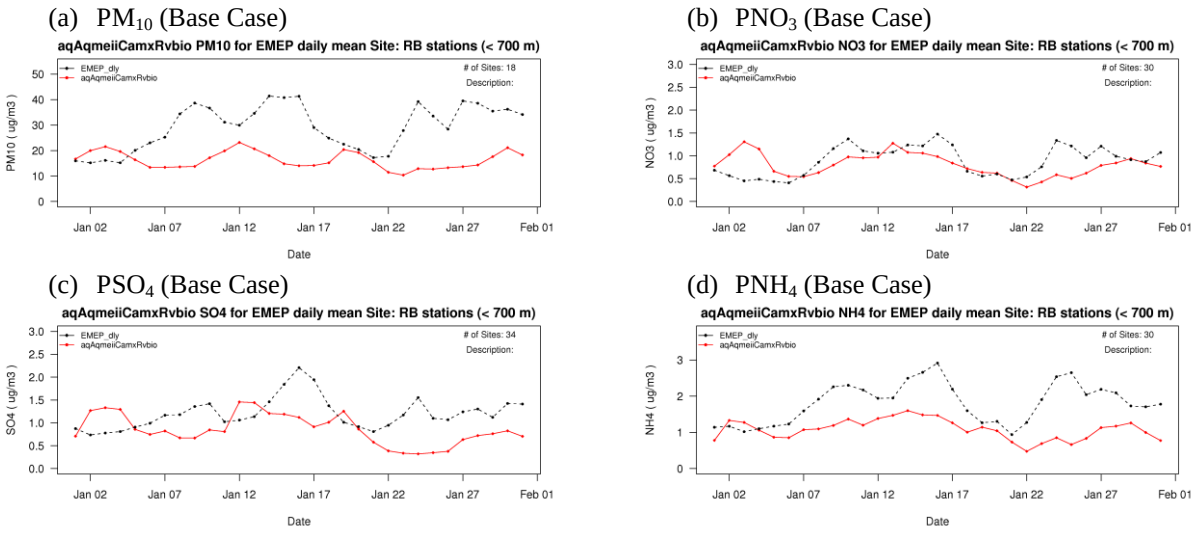

Figure S4. Modeled and observed daily mean concentrations of (a) PM_{10}, (b) PNO_3, (c) PSO_4, and (d) PNH_4 averaged over EMEP rural background stations for January 2006.

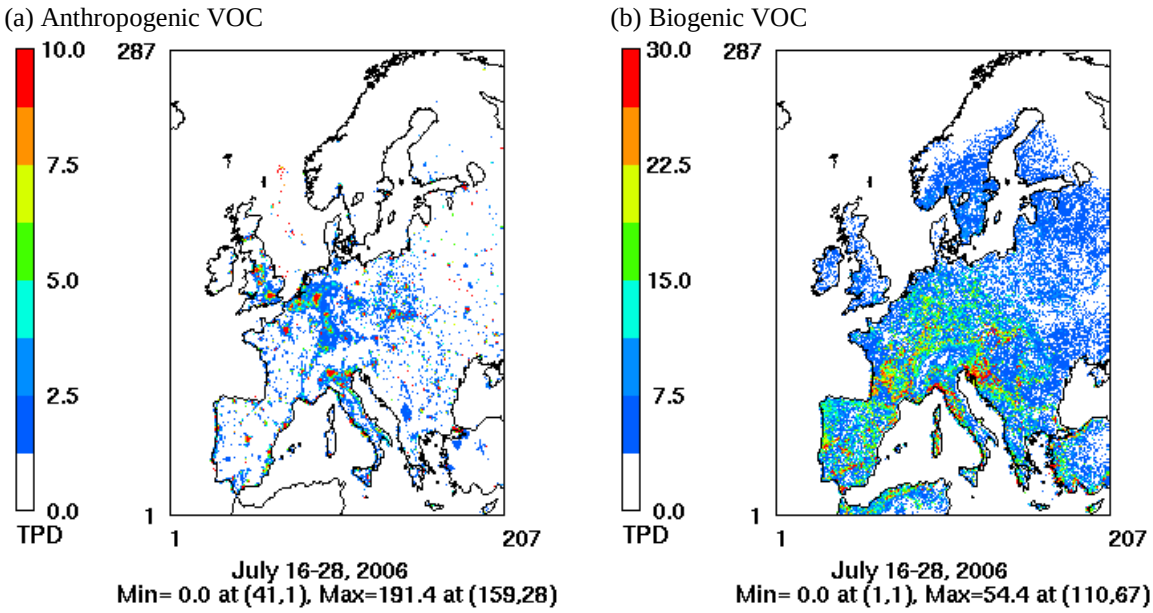

Figure S5. Episode average daily total VOC emissions from anthropogenic (a) and biogenic (b) sources.

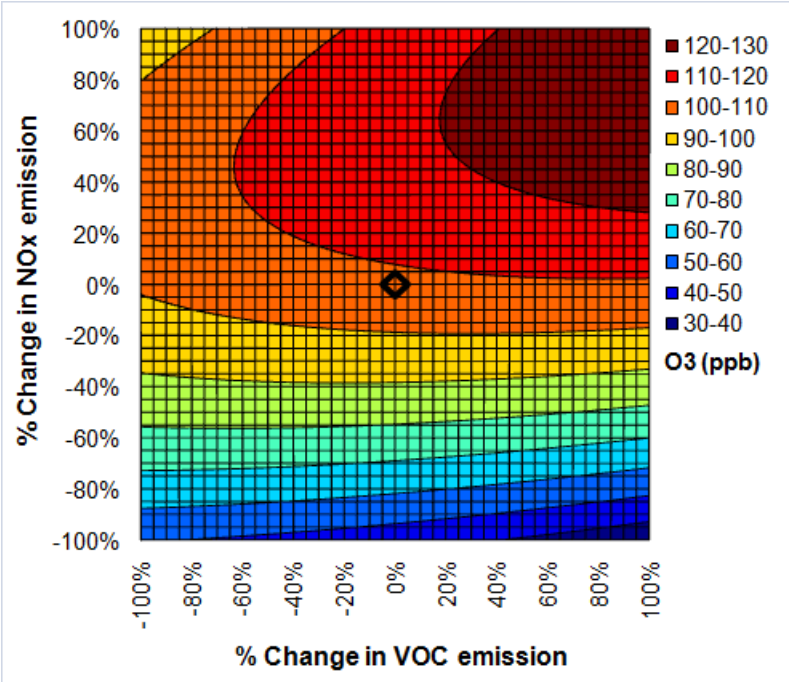

Figure S6. Ozone isopleths for episode average daily maximum ozone at Milano constructed using the first- and second-order sensitivity coefficients (Eq. (1)).